Journal of Solid State Chemistry 183 (2010) 425–430

Contents lists available at ScienceDirect

Journal of Solid State Chemistry

journal homepage: www.elsevier.com/locate/jssc

Cooperative effect of monoclinic distortion and sinusoidal modulation in the martensitic structure of Ni_2FeGa

J.B. Lu [a], H.X. Yang [a], H.F. Tian [a], L.J. Zeng [a], C. Ma [a], L. Feng [a], G.H. Wu [a], J.Q. Li [a,*], J. Jansen [b]

[a] Beijing National Laboratory for Condensed Matter Physics, Institute of Physics, Chinese Academy of Sciences, Beijing 100190, China
[b] National Center for HREM, Kavli Institute of Nanoscience, Delft University of Technology, 2628 CJ Lorentzweg 1, Delft, The Netherlands

ARTICLE INFO

Article history:
Received 18 August 2009
Received in revised form
22 November 2009
Accepted 7 December 2009
Available online 16 December 2009

Keywords:
Transmission electron microscopy
Ferromagnetic shape memory alloy
Ni_2FeGa
Cooperative effect
Multi-slice least-squares refinement

ABSTRACT

The structural features of the "5M" martensitic phase in Ni_2FeGa alloys have been determined by electron diffraction using the multi-slice least-squares (MSLS) method. The results demonstrate that the "5M" phase contains an evident cooperative effect of monoclinic distortion and sinusoidal modulation along the $[110]_c$ direction. Theoretical simulations based on our refined data suggest that the "5M" martensitic phase observed in Ni–Fe–Ga and Ni–Mn–Ga has visible common behaviors in both stacking sequence and local structural distortion. Considering the cooperative effect of monoclinic distortion and sinusoidal modulation, we demonstrate that the "7M" martensitic phase could adopt two equivalent structural phases corresponding with the stacking sequences of $(43)_2$ and $(5\bar{2})_2$, respectively.

1. Introduction

Ferromagnetic shape memory alloys showing a reversible structural phase transition have attracted great attention because of their potential applications as high sensitivity magnetic sensors and actuators [1–5]. Among a large number of alloys, Ni–Mn–Ga is a typical system which could give rise to maximum magnetic-field-induced strain (up to about 10%) [6]. However, the high brittleness of these alloys restricts the applications for the development of technologic devices. The Ni–Fe–Ga system as a new type of ferromagnetic shape memory alloys has been developed in order to improve toughness, it shows a notably better ductility than the Ni–Mn–Ga materials [7–9]. The stoichiometric Ni_2FeGa is a Heusler alloy with the well-defined $L2_1$ atomic order, which has a relatively high Curie temperature of about T_c=430 K, a martensitic transformation temperature of M_s=142 K, a saturated magnetization of 73 Am^2/kg and a low saturated field of 0.6 T. Moreover, this alloy exhibits a completely recoverable two-way shape memory effect with a strain of 0.3% upon the thermoelastic martensitic transformation [5]. The "5M" and "7M" structural modulations, corresponding to the well-known phonon anomalies in the $[\zeta\zeta 0]$ TA_2 branch, occur along the $[110]_c$ direction as characterized by TEM observations at low temperatures [10,11]. Structural analysis suggests that structural modulations in the layered martensitic structure show up certain common features as reported in Ni–Al [12], Ni–Al–Mn [13] and Ni–Mn–Ga [14]. In previous publications, two structural models have been proposed to interpret the structural properties in the martensitic structure, i.e. long-period modulation model with shuffling of the atomic $(110)_c$ basal planes and stacking sequences of the close-packed planes with a zigzag-like fault [15–20]. For example, the "5M" and the "7M" are denoted as $(32)_2$ and $(5\bar{2})_2$ stacking sequence ($(m\bar{n})_2$ indicates m planes shift in one direction, n planes shift in the opposite) in Zhdanov's notation, respectively. [12–15,20]. Actually, there is still ongoing debate about the atomic structural models corresponding with the superstructures, and certain interpretations for the observed structural features are apparently controversial. In the present paper, we will report on the structural studies of the "5M" and "7M" martensites. We will perform a crystal structure refinement for the "5M" martensitic phase of Ni_2FeGa as observed at low temperature. Based on the refined structural data, HRTEM simulations are carried out in comparison with the experimental results as reported in previous publications [20,21]. Structural analysis and HRTEM simulation for the "7M" martensitic phase are also discussed. The cooperative effect of monoclinic distortion and sinusoidal modulation is extensively studied.

2. Experimental

The Ni_2FeGa ribbon samples were synthesized by spinning the melt of the precursor ingot with a Ni_2FeGa composition, which

* Corresponding author. Fax: +86 10 62561422.
E-mail address: LJQ@aphy.iphy.ac.cn (J.Q. Li).

0022-4596/$ - see front matter Crown Copyright © 2009 Published by Elsevier Inc. All rights reserved.
doi:10.1016/j.jssc.2009.12.004

was prepared by melting pure metals in proportion in an induction furnace under argon atmosphere. Experimental details on the sample preparation and related characterization of physical properties have been reported in Ref. [5]. In order to avoid stress introduced from the grinding during TEM specimens preparation, 40 μm thick ribbons were selected and polished mechanically to about 20 μm, then ion-milled directly. Microstructure analyses were performed on an H-9000NA (300 kV) and a Tecnai F20 (200 kV) microscope both equipped with low-temperature sample stages to examine structural changes through the martensitic transformation. A DITABIS imaging plates (IPs) system was used to digitally record the electron diffraction patterns. The average probe size of the electron beam is around 50 nm in diameter. Structure refinements were performed using a software package MSLS [22], which performs a standard least-squares refinement in which the measured intensities of the diffracted beams are compared with those calculated using a multi-slice algorithm. It is shown that the atomic positions obtained by this MSLS procedure could have the same accuracy as those obtained from single-crystal X-ray diffraction [22,23].

3. Results and discussion

We firstly focus our attention on the martensitic structure of stoichiometric Ni_2FeGa in which the "5M" superstructure was commonly observed below martensitic transformation. Fig. 1 shows the electron diffraction patterns of the "5M" martensite Ni_2FeGa alloy taken along the $[001]_c$ (i.e. $[010]_m$) zone axis and $[1\bar{1}3]_c$ zone axis at the temperature of 100 K. The lattice parameters of the "5M" martensite can be determined from the main spots in the electron diffraction patterns. The resultant lattice parameters are a_m=4.0980(1) Å, b_m=5.4500(3) Å, c_m=20.4898(3) Å and β=88.4(1)°. The distance between two basal crystal planes along the modulation direction is determined to be 2.0482(2) Å for the "5M" phase at 100 K. In comparison with the parent $L2_1$ cubic phase, we obtain a value for the tetragonal ratio of $c/a \approx 0.9404$ which is associated with the value of achievable maximum strain, this data is fundamentally in consistent with previous results obtained in the "5M" and "7M" phases of Ni_2MnGa [24,25].

Fig. 2 shows a structural model for the "5M" martensitic structure, exhibiting a supercell consisting of 10 basal structural planes with the crystallographic axes as schematically illustrated, where $[100]_m$ is along $[110]_c$, $[010]_m$ is along $[001]_c$, and $[001]_m$ is slightly off $[110]_c$ (subscript "m" denotes the martensitic structure, and subscript "c" denotes the parent $L2_1$ cubic structure). The monoclinic angle in this structural model is determined from the electron diffraction of Fig. 1(a), as indicated as β=88.4(1)°. The long-period structural modulations in martensitic phases of Ni–Mn–Ga in general are accompanied with small displacements of atomic planes along either $[110]_c$ or $[1\bar{1}0]_c$ direction following a sinusoidal modulation as reported in [16–19,24,25]. It is also noted that the "5M" and "7M" martensitic structures commonly show visible monoclinic distortions as typically indicated in Fig. 1(a). Careful measurements suggest that this kind of monoclinic distortions could have a small alternation from one area to another in correlation with the local strain and defect structures. We therefore propose that the structural features of the "5M" phase should be interpreted by considering a cooperative effect of monoclinic distortion and sinusoidal modulation similar with what reported in Ref. [18,19] as schematically illustrated in the structural model of Fig. 2. In order to facilitate the structural refinement, we assume that the fractional coordinates of the atoms within the $(110)_c$ basal planes keep constant during the martensitic transformation [12–14,20]. In this case, we choose a Fourier series to describe the periodic harmonic displacements of the basal planes. The position, $\vec{x_z}$, of each basal plane z with a clear shift along $[1\bar{1}0]_c$

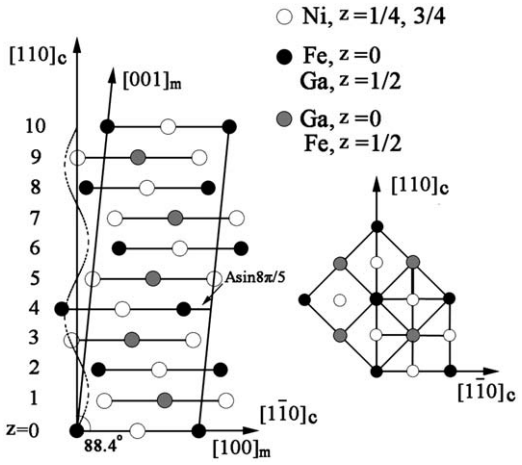

Fig. 2. Structural model of the "5M" martensite viewed along the $[001]_c$ (i.e. $[010]_m$) zone axis. The position of the basal plane z=4 is indicated by an arrow, the a_m is expanded doubly for clarity.

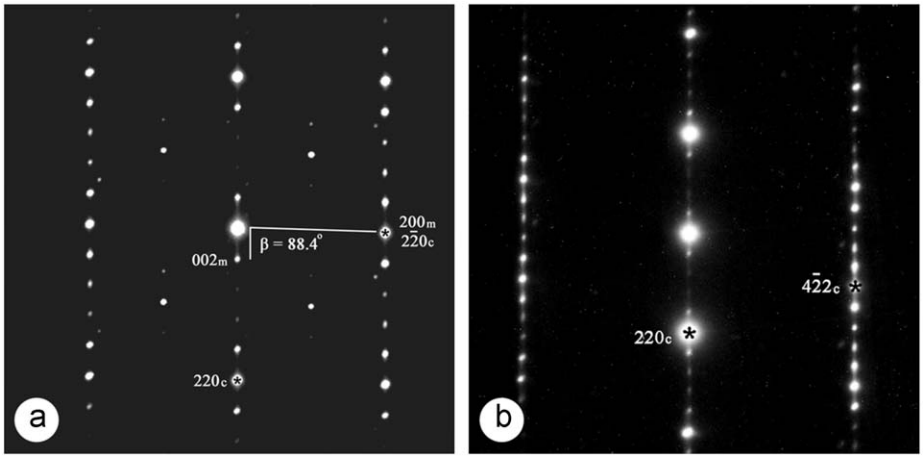

Fig. 1. Electron diffraction patterns of the "5M" martensite Ni_2FeGa alloy taken along (a) the $[001]_c$ (i.e. $[010]_m$) and (b) the $[1\bar{1}\bar{3}]_c$ zone axis direction at the temperature of 100 K.

or $[\bar{1}10]_c$ is given by

$$\overrightarrow{x_z} = \overrightarrow{x_{0z}} + \sum_{n=1}^{\infty}\left[A_n \sin\left(\frac{2n\pi z}{5}+\alpha\right)+B_n \cos\left(\frac{2n\pi z}{5}+\alpha\right)\right] \quad (z=\text{integer}) \tag{1}$$

where $\overrightarrow{x_{0z}} = d_{220} \times \tan(90^\circ - 88.4^\circ) \times z/a_m$ indicates the structural change of monoclinic distortion, which can be calculated from the lattice parameters and monoclinic angle obtained from the electron diffraction pattern. The Fourier terms indicate the periodic modulation of basal planes and the index n defines the order of the Fourier series. α is the initial phase of the periodic modulation wave. It will be noted in the following text that α plays an important role in determining the relative shift between two neighboring basal planes. In previous literature, it is demonstrated that the amplitude of the atomic displacements arising from the first-order harmonic function was fundamentally good enough for theoretical analysis of the diffraction results in Ni–Mn–Ga system [18,19]. Hence, in the following discussion, we will only consider the first order in the Fourier series. The symmetry rules only permit the refinement of the $A_n \sin(2n\pi z/5+\alpha)$ terms in Eq. (1), thus the position of each basal plane z is simply given by

$$\overrightarrow{x_z} = \overrightarrow{x_{0z}} + A\sin\left(\frac{2\pi z}{5}+\alpha\right) \quad (z=\text{integer}) \tag{2}$$

where A indicates the amplitude of sinusoidal modulation wave. The $A\sin(2\pi z/5+\alpha)$ term defines the position of basal plane z in the supercell governed by the sinusoidal modulation. The initial phase α of sinusoidal modulation wave is adopted to be 0. As an example, the calculated basal plane position for z=4 is written as $A\sin(8\pi/5)$ and indicated by an arrow in Fig. 2.

A monoclinic supercell, with the space group $I2/m$ and the lattice parameters of a_m=4.0980(1) Å, b_m=5.4500(3) Å, c_m=20.4898(3) Å and β=88.4(1)°, is used for structural refinement as shown in Fig. 2. The atomic temperature factors are assumed to be isotropic, all crystallographic data are presented in Table 1.

Table 2 exhibits the coordinates of the positions of the 10 basal planes in the monoclinic supercell. Table 3 gives the five sets of experimental data of electron diffraction. The R value used in our refinement is defined as $R = \sum[(I_{obs})-(I_{cal})]^2 / \sum(I_{obs})^2$. All reflections with $I_{obs} > 2\sigma(I_{obs})$ are used in the present calculations, where $\sigma(I_{obs})$ is the standard deviation of the diffraction intensity. Experimental diffraction pattern used in our refinement were obtained by using an incident electron beam with a small convergence angle, such that the illumination is similar to a plane wave and sharp diffraction spots could be obtained. The intensity of each reflection is measured by integrating over a circular area around each diffraction spot. A small spot size (~50 nm) was used for electron diffraction in order to have a relatively small variation of thickness and crystal orientation, and to reduce the amount of unwanted information, e.g. impurities and structural defects. Firstly, the scale factor, crystal misorientation and thickness for each electron diffraction pattern were refined. Five sets of experimental data were taken to have a range of thicknesses. The overall R value for these sets is about 4.663%. From the coordinates of the 10 basal planes in the monoclinic supercell, the amplitude of sinusoidal modulation wave,A, is estimated to be about 0.0840, therefore the real amplitude of the modulation wave is expected to be around 0.3442 Å. According to the theoretical studies for the shape memory alloys, the modulation amplitudes in the two atomic layers in Ni_2MnGa have different values of 0.292 and 0.324 Å for the Mn–Ga and Ni planes, respectively [25], these data are fundamentally consistent with our refined results.

Table 1
Crystallographic data for the "5M" martensitic superstructure at 100 K.

Crystal system					Monoclinic
Space group					*I2/m*
a (Å)					4.0980
b (Å)					5.4500
c (Å)					20.4898
β (°)					88.4
Atom type	Wyck.	*x*	*y*	*z*	B (Å2)
Ni1	8j	0.0799	0.2500	0.1000	0.34
Ni2	8j	0.5494	0.2500	0.2000	0.34
Ni3	4h	0.5000	0.2500	0	0.34
Fe1	2a	0	0	0	0.27
Fe2	4i	0.0799	0	0.6000	0.27
Fe3	4i	0.0494	0	0.2000	0.27
Ga1	2b	0	0.5000	0	0.36
Ga2	4i	0.5494	0	0.7000	0.36
Ga3	4i	0.5799	0	0.1000	0.36

The atomic temperature factors are assumed to be isotropic.

Table 2
Coordinates of basal planes along the $[1\bar{1}0]_c$ direction in the monoclinic unit cell.

Plane *z*	0	1	2	3	4	5
x	0	0.0799	0.0494	0.9506	0.9201	0
Plane *z*	6	7	8	9	10	
x	0.0799	0.0494	0.9506	0.9201	0	

Table 3
Experimental data of the electron diffraction sets used for the structure refinement.

Zone axis	No. of reflections	Thickness (nm)	Center of Laue circle			*R* value (%)
			h	*k*	*l*	
$[010]_m$	320	17.0(4)	−0.11(5)	0.000	2.78(4)	5.9
$[010]_m$	336	5.2(7)	0.27(7)	0.000	−0.45(7)	6.9
$[010]_m$	306	26.7(7)	0.08(5)	0.000	−1.97(3)	1.7
$[010]_m$	333	12.6(4)	0.17(8)	0.000	−0.50(9)	6.3
$[010]_m$	312	6.4(9)	0.11(3)	0.000	−0.76(4)	7.9

The overall R value is 4.663%. In the present work, we use the data taken from five crystal areas with different thickness. The misorientation of the crystal is given as the center of the Laue circle in the electron diffraction pattern in Miller indices h, k, and l as illustrated for each pattern.

The selected bond lengths of the "5M" martensitic phase obtained in our study corresponding to crystallographic data presented in Table 1 are listed in Table 4, in which certain structural data of the parent $L2_1$ cubic structure are also displayed for comparison [5]. It is clearly recognizable that the bond lengths become remarkably diverse in the "5M" martensitic phase, suggesting that a complex structural change appears in association with the martensitic transformation in this kind of materials.

Fig. 3 exhibits the major structure changes of the Fe sub-lattice through the martensitic transformation. It is commonly accepted that the Fe sub-lattice plays a critical role for understanding the magnetic properties in this kind of materials [26,27]. Fig. 3(a) illustrates a tetragonal Fe sub-lattice in the parent $L2_1$ cubic phase with parameters $a_{Fe}=c_{Fe}$=4.0591 Å, b_{Fe}=5.7405 Å and β=90° [5], in which the Ni and Ga atom are neglected. Fig. 3(b) displays the projection of this tetragonal structure along the $[001]_c$ direction, and Fig. 3(c) illustrates the projection of the deformed tetragonal structure along $[001]_c$ direction for the MT phase with lattice parameters of a_{Fe}=4.0980(1) Å, b_{Fe}=5.4500(3) Å, c_{Fe}=4.1090(1) and β=85.6(4)°. The visible structural differences between

Fig. 3(b) and (c) suggest that the martensitic transformation occurring in the present system could evidently influence the magnetic property in this kind of system.

Actually, the long-period martensitic structures, such as "5M" and "7M", commonly appear in a variety types of Heusler alloys. For instance, certain Ni–Mn–Ga samples with specific compositions show clear superstructures at room temperature, which allows the performance of the HRTEM observations and directly reveal the atomic structures for the long-period martensitic phases [20,21]. A careful analysis suggests that the structural data obtained in our previous refinements can be used to interpret the main structural features of the "5M" HRTEM image obtained in Ni–Mn–Ga system. Our image simulation has been performed with the JEMS software (developed by Prof. P. Stadelmann) using the multi-slice method. Fig. 4 shows a theoretical HRTEM image for the "5M" martensite along the $[001]_c$ (i.e. $[010]_m$) zone axis. The atomic positions from the structural model are superimposed on the image. It is recognizable that the $(32)_2$ stacking sequence shows very similar behaviors with the data reported by Pons et al. in Ni–Mn–Ga for the "5M" modulation structure [20,21].

In order to understand the structural features observed in the martensitic phase, a debate between the modulation model and the stacking sequence model has persisted for decades [12–20]. In

Table 4
Selected bond lengths of the parent $L2_1$ cubic structure and the martensitic structure.

Cubic (Å)		Martensite (Å)		
Fe–Fe	4.059	Fe1–Fe1	$4.098_{\times 2}$	
		Fe1–Fe2	$3.794_{\times 6}$	$4.188_{\times 6}$
		Fe1–Fe3	$4.109_{\times 2}$	
Ga–Ga	4.059	Ga1–Ga1	$4.098_{\times 2}$	
		Ga1–Ga2	$4.109_{\times 3}$	
		Ga1–Ga3	$4.188_{\times 5}$	$3.794_{\times 6}$
Ni–Ni	2.870	Ni1–Ni1	$2.725_{\times 2}$	
		Ni1–Ni2	2.850	$2.945_{\times 2}$
		Ni1–Ni3	$2.639_{\times 2}$	$3.181_{\times 3}$
Fe–Ga	2.870	Fe1–Ga1	$2.725_{\times 2}$	
		Fe2–Ga2	2.850	$2.945_{\times 2}$
		Fe3–Ga3	$2.850_{\times 2}$	
Ni–Fe	2.486	Ni1–Fe1	$2.490_{\times 4}$	
		Ni1–Fe2	$2.461_{\times 6}$	
		Ni1–Fe3	$2.461_{\times 2}$	
Ga–Ni	2.486	Ga1–Ni1	$2.490_{\times 4}$	
		Ga2–Ni2	$2.461_{\times 6}$	$2.484_{\times 3}$
		Ga3–Ni3	$2.490_{\times 3}$	

The bond lengths of the parent $L2_1$ cubic structure are calculated with parameter a=5.7405 Å as reported in Ref. [5].

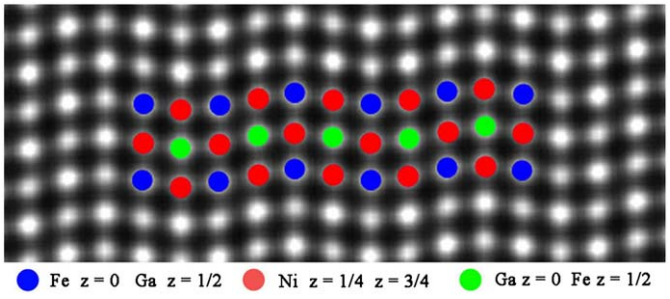

Fig. 4. Simulated HRTEM image of the "5M" martensite along the $[001]_c$ (i.e. $[010]_m$) zone axis, with a thickness of 2.3 nm and a defocus of −54 nm. The projected atomic positions from the structural model are superimposed on the image.

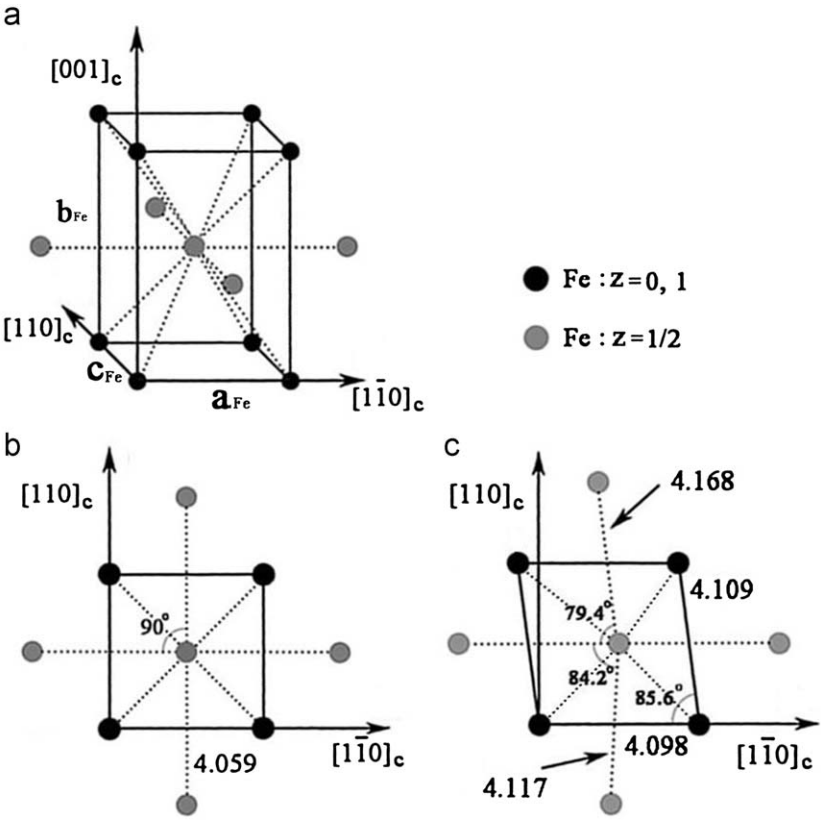

Fig. 3. Schematic representations of alternations of the Fe sub-lattice through the martensitic transformation. (a) The structural model of the parent $L2_1$ cubic phase. (b) The projection of the parent phase along the $[001]_c$ direction. (c) The $[001]_c$ projection of the deformed tetragonal structure below MT.

particular, it has been demonstrated that the "5M" martensite can be well interpreted by a modulation model in the orthorhombic unit cell, on the other hand, the $(32)_2$ stacking sequence model can quantitatively interpret the monoclinic distortion, in which the monoclinic angle (β) was considered to be determined by shift parameters and stacking sequence [14]. In what follows, we show that the monoclinic distortion and sinusoidal modulation should be considered cooperatively for understanding the "5M" and "7M" modulated structures. As displayed above, the cooperative effect of monoclinic distortion and sinusoidal modulation can interpret the arrangement of the $(32)_2$ stacking sequence in "5M" martensitic structure reasonably.

Pons et al. argued in previous literature that, for the "7M" layered martensite, the experimental observations show visible disagreement with the structural model based on the wave-like modulation which could only exhibits the $(43)_2$ stacking sequence [20]. In the present study, we apply the cooperative structural model of monoclinic distortion and sinusoidal modulation to analyze the "7M" layered martensite. Because we did not observe the "7M" martensitic phase in the sample used in the present study, we use the structural data for martensitic Ni_2MnGa as reported in Ref. [14], i.e. a_m=0.426 nm, b_m=0.543 nm, c_m=2.954 nm and β=94.3°, and the vertical distance between two basal plane is given by $c_m \sin\beta/14$=0.21 nm. It is noted that the modulation amplitudes reported in layered martensite is in the range of 0.06 and 0.09 [13,14,18,25], thus we adopted the A=0.0840. As mentioned in above context, we found that two degenerate states corresponding with the initial phase α being π and 0 could both give rise to reasonable martensitic phases as illustrated in Fig. 5. For the "7M" martensitic phase supercell with the initial phase $\alpha=\pi$, the position of each basal plane z is simply given by Eq. (3). Fig. 5(a) shows the corresponding cooperative structural model. The calculated positions of the 14 basal planes according to Eq. (3) are listed in Table 5. Fig. 5(c) shows the simulated image of "7M" structure along the $[001]_c$ (i.e. $[010]_m$) zone axis following the structural model of Fig. 5(a).

$$\overrightarrow{x_z} = \overrightarrow{x_{0z}} + A\sin\left(\frac{2\pi z}{7} + \pi\right) \quad (z = \text{integer}) \tag{3}$$

It is clearly recognizable in Fig. 5(c) and Table 5 that the cooperative effect in the "7M" matensitic supercell with the initial phase $\alpha=\pi$ yields a $(43)_2$ stacking sequence, in which four

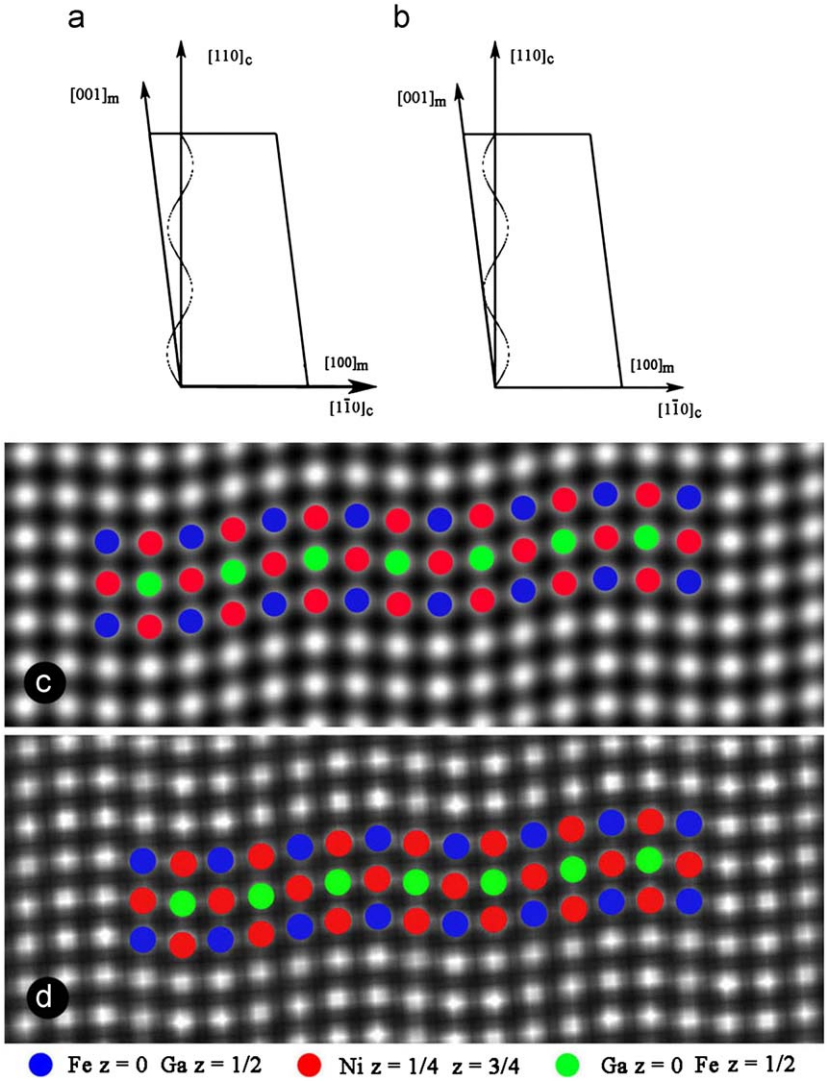

Fig. 5. (a) Schematic representation of the cooperative structural model for the initial phase $\alpha=\pi$, (b) schematic representation of the cooperative structural model for α=0, (c) simulated HRTEM image of the "7M" martensite along the $[001]_c$ (i.e. $[010]_m$) direction with a thickness of 2.0 nm and a defocus of −30 nm and (d) simulated HRTEM image of the "7M" martensite along the $[001]_c$ (i.e. $[010]_m$) zone axis corresponding to (b), with a thickness of 2.2 nm and a defocus of −44 nm. The projected atomic positions from the structural model are superimposed on the images, respectively.

Table 5
Coordinates of basal planes in the "7M" martensite with the initial phase α being π.

Plane z	0	1	2	3	4
x	0	−0.1026	−0.1561	−0.1477	−0.1117
Plane z	5	6	7	8	9
x	−0.1035	−0.1568	−0.2594	−0.3622	−0.4155
Plane z	10	11	12	13	14
x	−0.4070	−0.3714	−0.3629	−0.4162	−0.5190

The amplitude of sinusoidal modulation wave A is 0.0840.

Table 6
Coordinates of basal planes in the "7M" martensite with the initial phase α being 0.

Plane z	0	1	2	3	4
x	0	0.0286	0.0077	−0.0746	−0.1847
Plane z	5	6	7	8	9
x	−0.2671	−0.2880	−0.2594	−0.2308	−0.2516
Plane z	10	11	12	13	14
x	−0.3343	−0.4441	−0.5268	−0.5474	−0.5190

The amplitude of sinusoidal modulation wave A is 0.0840.

basal planes shift in one direction and the three others shift in the opposite direction.

Furthermore, we can also obtained another "7M" martensitic structure from the cooperative structural model with the initial phase α=0 as schematically illustrated in Fig. 5(b). The coordinates of the 14 basal planes are listed in Table 6. HRTEM image simulation along the $[001]_c$ (i.e. $[010]_m$) zone axis direction (Fig. 5(d)) exhibits a clear $(52)_2$ stacking sequence in which five planes shift in one direction and the two other planes shift in the opposite direction. These facts suggest that the $(43)_2$ and $(52)_2$ stacking sequences could be the two typical types of martensitic structures originating from the cooperative effect of monoclinic distortion and sinusoidal modulation for the "7M" structure.

In addition, it is also noted in previous publications that much more complex stacking sequences in the martensitic phases were also obtained such as $(75)_2$, $(55)_2$ [14,21] and (5232) [13], and these structures likely arise from the irregular intergrowth of different modulated phases with visible monoclinic distortion. Moreover, these complex stacking sequences observed by HRTEM can be also interpreted from cooperative effect of monoclinic distortion and several modulation waves with different amplitudes, initial phases and periodicities. For instance, Martynov et al. reported that the shear modulation in martensitic lattice can be considered as superimposition of static displacement waves with the following propagation and polarization vectors: $k_{1,2,3}\|[110]$, $e_{1,2,3}\|[1\bar{1}0]$, $|k_1|=4\pi/5a\sqrt{2}$, $|k_2|=8\pi/5a\sqrt{2}$, $|k_3|=12\pi/5a\sqrt{2}$, $|e_1|\cong a\sqrt{2}/17$, $|e_2|\cong a\sqrt{2}/500$, $|e_3|=a\sqrt{2}/150$ [16,17].

4. Conclusions

In summary, the "5M" martensitic structure in Ni_2FeGa at 100 K was studied by means of *in-situ* TEM observation and refined using the multi-slice least-squares method. The *in-situ* TEM studies reveal a clear structural phase transition related to martensitic transformation at about 142 K. The "5M" martensitic structure can be well interpreted as a cooperative effect of monoclinic distortion and sinusoidal modulation along the $[110]_c$ direction. The structure refinement based on the cooperative model demonstrates that the amplitude of the sinusoidal modulation wave is 0.3442 Å, and the monoclinic angle β is about 88.4(1)°. Furthermore, the simulated HRTEM image of "5M" phase based on the refined structure data exhibits a $(3\bar{2})_2$ stacking sequence. Considering the cooperative effect of monoclinic distortion and sinusoidal modulation, we demonstrate that the "7M" layered martensite could have two equivalent structural phases corresponding with the stacking sequences of $(43)_2$ and $(5\bar{2})_2$ in which the initial phase of modulation wave being π and 0, respectively.

Acknowledgments

The work reported here is supported by the National Natural Foundation of China, Chinese Academy of Sciences and the Ministry of Science and Technology of China.

References

[1] P.J. Webster, K.R.A. Ziebeck, S.L. Town, M.S. Peak, Philos. Mag. B 49 (1984) 295–310.
[2] R. Tickle, R.D. James, T. Shield, M. Wutting, V.V. Kokorin, IEEE. Trans. Magn. 35 (1999) 4301–4310.
[3] R.D. James, M. Wuttig, Philos. Mag. A 77 (1998) 1273–1299.
[4] K. Oikawa, L. Wulff, T. Iijima, F. Gejima, T. Ohmori, A. Fujita, K. Fukamichi, R. Kainuma, K. Ishida, Appl. Phys. Lett. 79 (2001) 3290–3292.
[5] Z.H. Liu, M. Zhang, Y.T. Cui, Y.Q. Zhou, W.H. Wang, G.H. Wu, Appl. Phys. Lett. 82 (2003) 424–426.
[6] A. Sozinov, A.A. Likhachev, N. Lanska, K. Ullakko, Appl. Phys. Lett. 80 (2002) 1746–1748.
[7] F. Alvarado-Hernandez, D.E. Soto-Parra, R. Ochoa-Gamboa, P.O. Castillo-Villa, H. Flores-Zuniga, D. Rios-Jara, J. Alloys. Compd. 462 (2008) 442–445.
[8] J.M. Barandiaran, J. Gutierrez, P. Lazpita, V.A. Chernenko, C. Seguic, J. Pons, E. Cesari, K. Oikawa, T. Kanomata, Mater. Sci. Eng. A 478 (2008) 125–129.
[9] K. Oikawa, T. Ota, T. Ohmori, Y. Tanaka, H. Morito, A. Fujita, R. Kainuma, K. Fukamichi, K. Ishida, Appl. Phys. Lett. 81 (2002) 5201–5203.
[10] H.R. Zhang, C. Ma, H.F. Tian, G.H. Wu, J.Q. Li, Phys. Rev. B 77 (2008) 2141061–21410612.
[11] J.Q. Li, Z.H. Liu, H.C. Yu, M. Zhang, Y.Q. Zhou, G.H. Wu, Solid State Commun. 126 (2003) 323–327.
[12] Y. Noda, S.M. Shapiro, G. Shirane, Y. Yamada, L.E. Tanner, Phys. Rev. B 42 (1990) 10397–10404.
[13] S. Morito, K. Otsuka, Mater. Sci. Eng. A 208 (1996) 47–55.
[14] J. Pons, V.A. Chernenko, R. Santamarta, E. Cesari, Acta Mater. 48 (2000) 3027–3038.
[15] G.S. Zhdanov, Dokl. Akad. Nauk. SSSR 48 (1945) 39–43.
[16] V.V. Martynov, V.V. Kokorin, J. de Phys. III France 2 (1992) 739–749.
[17] V.V. Martynov, J. de Physique. IV 5 (1995) C8-91-100.
[18] L. Righi, F. Albertini, L. Pareti, A. Paoluzi, G. Calestani, Acta Mater. 55 (2007) 5237–5245.
[19] L. Righi, F. Albertini, G. Calestani, L. Pareti, A. Paoluzi, C. Ritter, P.A. Algarabel, L. Morellon, M. Ricardo Ibarra, J. Solid State Chem. 179 (2006) 3525–3533.
[20] J. Pons, R. Santamarta, V.A. Chernenko, E. Cesari, J. Appl. phys. 97 (2005) 0835161–0835167.
[21] J. Pons, R. Santamarta, V.A. Chernenko, E. Cesari, Mater. Sci. Eng. A 438–440 (2006) 931–934.
[22] J. Jansen, D. Tang, H.W. Zandbergen, H. Schenk, Acta cryst. A 54 (1998) 91–101.
[23] J. Jansen, H.W. zandbergen, Ultramicroscopy 90 (2002) 291–300.
[24] A.T. Zayak, P. Entel, Mater. Sci. Eng. A 378 (2004) 419–423.
[25] A.T. Zayak, P. Entel, J. Enkovaara, A. Ayuela, R.M. Nieminen, J. Phys.: Condens. Matter 15 (2003) 159–164.
[26] Z.H. Liu, H.N. Hu, G.D. Liu, Y.T. Cui, M. Zhang, J.L. Chen, G.H. Wu, Phys. Rev. B 69 (2004) 1344151–1344156.
[27] J. Kubler, A.R. Williams, C.B. Sommers, Phys. Rev. B 28 (1983) 1745–1755.